Fluorescence Imaging

DOI: 10.1002/ange.201206749

In Situ Probing of Newly Synthesized Peptidoglycan in Live Bacteria with Fluorescent D-Amino Acids**

Erkin Kuru, H. Velocity Hughes, Pamela J. Brown, Edward Hall, Srinivas Tekkam, Felipe Cava, Miguel A. de Pedro, Yves V. Brun, and Michael S. VanNieuwenhze**

Bacterial growth is controlled by the peptidoglycan (PG) cell wall, a rigid and essential structure composed of glycan strands cross-linked by D-amino acid (DAA)-containing short peptides, the biosynthesis machinery of which is a high-value target for antibiotics.[1] Despite the incredible importance of this polymer, our knowledge of PG dynamics has been severely hampered by the lack of a global strategy for direct imaging of sites of PG synthesis in live cells. Limitations of current labeling methods, such as toxic effects and poor membrane permeability of the probes, have limited their applicability to only a small set of bacterial species.[2] Commonly, these methods are labor-intensive and their sensitivity suffers from their indirect and multiple-step nature. To overcome these limitations, we sought a chemical biology approach that would enable the rapid and covalent incorporation and detection of a fluorescently derivatized PG component during cell wall synthesis in real time, in a wide range of bacterial species, and in live cells.

Given the recently established role of the PG biosynthetic machinery in incorporating various natural DAAs in the PG of diverse bacteria,[3] we hypothesized that the mechanisms[3b] for DAA incorporation in PG are common to the bacterial domain but still highly selective, and that molecules with various functionalities could be incorporated into the sites of new PG synthesis if these molecules are attached to a DAA backbone. To test this hypothesis, we attached the relatively small fluorophores, 7-hydroxycoumarin-3-carboxylic acid (HCC-OH) and 4-chloro-7-nitrobenzofurazan (NBD-Cl), to a D-amino acid backbone, 3-amino-D-alanine, by using a modular and simple synthetic scheme, and generated the fluorescent amino acids HADA (emission maximum 450 nm, blue) and NADA (emission maximum 538 nm, green; Scheme 1 and Figure S2 in the Supporting Information).

Growth of the phylogenetically diverse model species *Escherichia coli*, *Agrobacterium tumefaciens*, and *Bacillus subtilis* in the presence of these fluorescent D-amino acids (FDAAs) for as little as one generation (Figure S1a in the Supporting Information) resulted in strong peripheral and septal labeling of entire cell populations (Figure 1 and Figure S3a in the Supporting Information, upper panels) without affecting growth rate (Figure S3b in the Supporting Information). Neither of the fluorescent L-amino acids (FLAAs, prepared from 3-amino-L-alanine, Figure S2c in the Supporting Information) resulted in significant labeling (Figure S3c), thus indicating that labeling is specific to the D-enantiomers. The labeling was exclusive to viable cells treated with the FDAAs and was not the result of nonspecific interaction of FDAAs with the PG (Figure S4 in the Supporting Information). Moreover, incorporation did not occur into teichoic acids for *B. subtilis* as indicated by identical labeling of wild-type and a Δ*dltA* mutant that does not incorporate D-alanine into its teichoic acids (Figure S5a, b in the Supporting Information).

Retained fluorescence on the purified sacculi (Figure 1 and Figure S3a in the Supporting Information, lower panels)

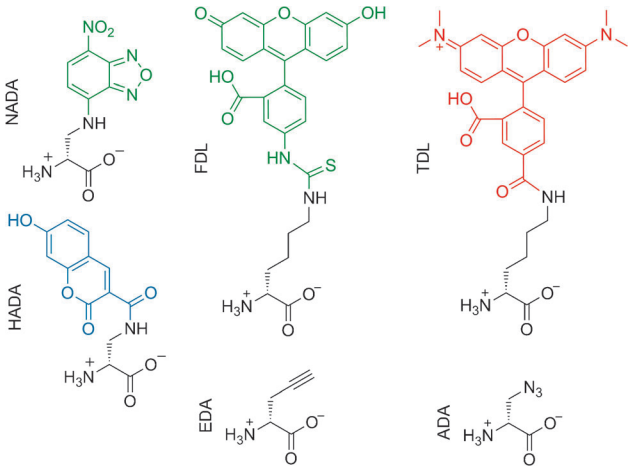

Scheme 1. Structures of the fluorescent D-amino acids HADA, NADA, FDL, and TDL with the fluorescent group shown in the color of the fluorophore (blue, green, and red) and the "clickable" D-amino acids EDA and ADA.

[*] E. Kuru, H. V. Hughes, Dr. P. J. Brown, E. Hall, S. Tekkam, Prof. Y. V. Brun, Prof. M. S. VanNieuwenhze
Indiana University
Bloomington, IN 47405 (USA)
E-mail: ybrun@indiana.edu
mvannieu@indiana.edu
Prof. F. Cava, Prof. M. A. de Pedro
Universidad Autonoma de Madrid, Campus de Cantoblanco
Madrid, 28049 (Spain)

[**] We thank David Kysela for discussions and critical reading of the manuscript, Bill Turner and Alvin Kalinda for their help in simplifying the synthesis of FDAAs and Prof. Patricia Foster and the members of her laboratory for their support during the initial stages of the project. M.S.V. was funded by National Institutes of Health (NIH) grant AI 059327, Y.V.B. by NIH grant GM051986, M.A.P. by Ministry of Education and Science (Spain) grant BFU2006-04574 and by the Fundación Ramón Areces, F.C. by MICINN (Spain) grant RYC-2010-06241, and P.J.B. by NIH National Research Service Award AI072992.

Supporting information for this article is available on the WWW under http://dx.doi.org/10.1002/anie.201206749.

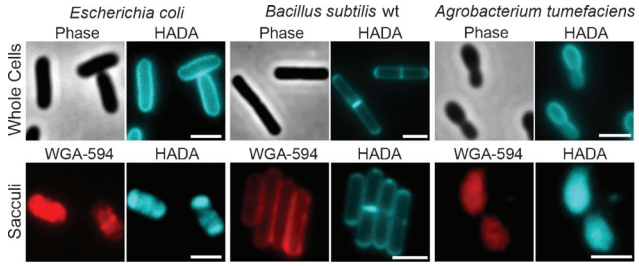

Figure 1. Long labeling pulses with HADA uniformly label PG in live cells of *E. coli*, *B. subtilis*, and *A. tumefaciens*. The FDAA fluorescence is retained in isolated sacculi, which are also stained with the *N*-acetylglucosamine (GlcNAc) specific WGA lectin conjugated to Alexa Fluor 594 (red). Scale bars: 2 μm.

demonstrated that the labeling of PG by the FDAAs was covalent. HPLC analyses of muropeptides isolated from labeled cells (Figure 2a–c, Figures S6 and S7 in the Supporting Information) revealed that 0.2–2.8% of total muropeptides were modified (Figure 2c), which is sufficient for detection in various experiments while avoiding possible toxicity issues that could result from abundant incorporation. Significantly, the FDAA-specific peaks, which were absent in samples treated with FLAAs, could be distinguished from unlabeled muropeptides at FDAA-specific absorption wavelengths (Figure 2b). MS/MS analyses of FDAA-modified muropeptides in *B. subtilis* indicated that FDAAs were exclusively incorporated in the fifth position of the stem peptide (Figure 2d, Figure S7a,d and Table S1 in the Supporting Information). Interestingly, in a *ΔdacA* mutant of *B. subtilis*, the fraction of labeled muropeptides and the fluorescent signal were substantially higher than in wild-type *B. subtilis*. The diminshed signal intensity in wild-type cells is likely due to the D,D-carboxypeptidase activity of DacA (Figure S5c,d in the Supporting Information). In contrast, the detectable incorporation was solely at the fourth position in *E. coli* and *A. tumefaciens* (Figure 2d and Figure S7 in the Supporting Information). These results are in agreement with the known sites of incorporation of various natural DAAs in these species and suggest that, similar to DAAs, FDAAs incorporate mainly through periplasmic exchange reactions with the muropeptides; these reactions are catalyzed either by D,D-transpeptidases, for example, in *B. subtilis*, or by L,D-transpeptidases, for example, in *E. coli* and *A. tumefaciens*.[3b,4] This DAA-like behavior together with the ease of fluorescent detection make FDAAs a strong alternative to radioactive probes for studying activities of PG synthesis enzymes in vitro[3c] and in vivo[5].

In contrast to current approaches,[2b,f] pulse–chase experiments with HADA allowed the real-time tracking of new PG incorporation during growth by time–lapse microscopy. In *E. coli* and *B. subtilis ΔdacA* (Figure 3a and Movies 1 and 2 in the Supporting Information), the polar caps retained the HADA signal, but the signal from the lateral walls dispersed as the cells grew; this observation is in agreement with reports of cell wall growth along the length of the lateral walls.[2f,5]

Strikingly, short labeling times (2–8% of doubling time) using *E. coli* and *B. subtilis ΔdacA* with HADA resulted in preferential localization of the signal at the septal plane of predivisional cells and in punctate patterns on the lateral walls of elongating cells (Figure 4). Super-resolution microscopy of *E. coli* revealed reticulated hoop-like patterns of HADA labeling around the lateral wall (Figure 3b and Movie 3 in the Supporting Information); these patterns support the finding of locations with a high density of PG in the side walls.[6] This ability of FDAAs to resolve insertion of new PG enables the first direct detection of zones of PG synthesis in a structured pattern rather than in a random pattern in *E. coli*; this result is consistent with recent reports describing the

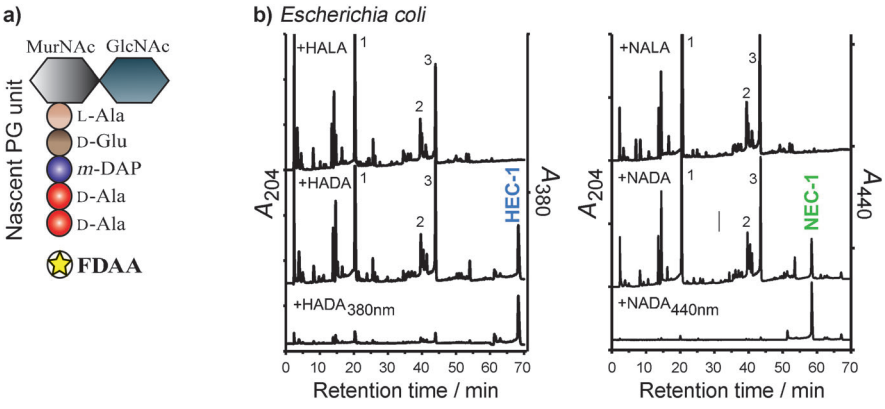

c)

Strain and treatment	Mod. PG
B. subtilis ΔdacA + HADA	2.1%
B. subtilis wt + NADA	0.2%
E. coli + HADA	2.8%
E. coli + NADA	1.9%
A. tumefaciens + HADA	2.5%

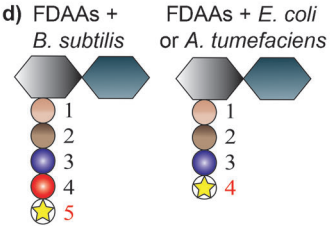

Figure 2. FDAA incorporation into the stem peptide of the PG subunit. a) Schematic representation showing the muramylpentapeptide precursor unit. b) HPLC detection of modified muropeptides in *E. coli* incubated with HADA or HALA and NADA or NALA. Samples were monitored using a dual-wavelength UV monitor set for general muropeptide detection and for FDAA-specific wavelengths. Peaks HEC-1 and NEC-1 correspond to the HADA- or NADA-modified muropeptides in *E. coli* and were further characterized by electrospray ionization MS/MS (ESI–MS/MS). The numbers 1–3 in the chromatograms assign the peaks to the peptides of the respective lengths. c) Percentage of FDAA incorporation into the total muropeptides varies among different bacteria as revealed by HPLC analysis. d) MS/MS analyses show that FDAAs exclusively incorporate into the 4th position of muropeptides in *E. coli* and *A. tumefaciens* and the 5th position in *B. subtilis*. See also Figures S6,7 and Table S1 in the Supporting Information. MurNAc = N-acetylmuramic acid; *m*-DAP = *meso*-diaminopimelic acid.

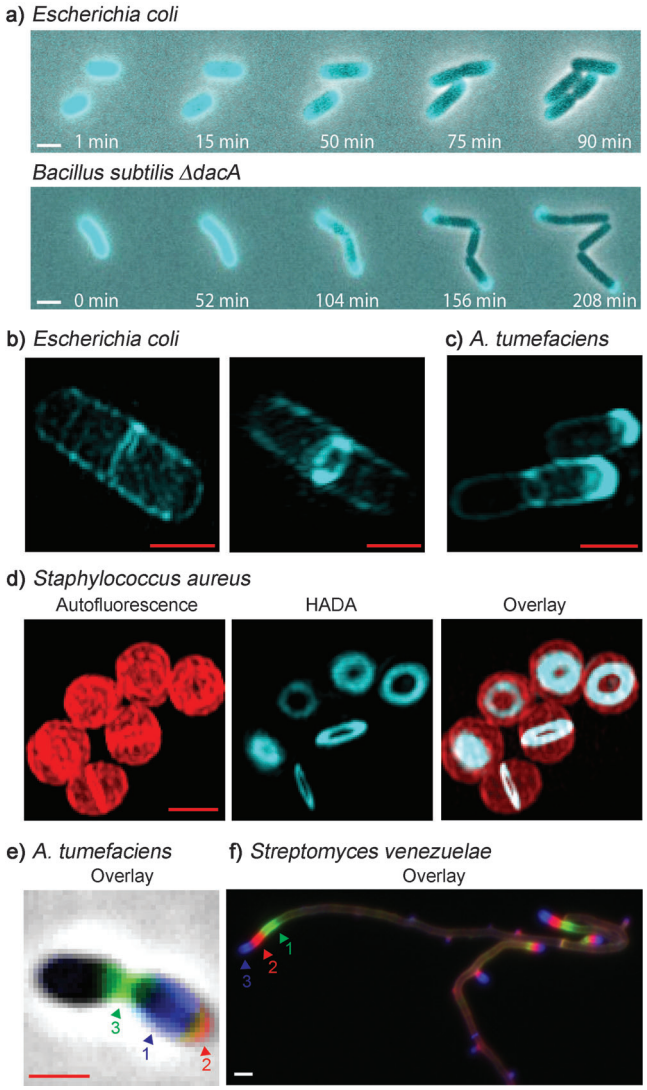

Figure 3. FDAAs label diverse bacterial growth patterns. a) Time-lapse microscopy of HADA-labeled *E. coli* and *B. subtilis ΔdacA* cells imaged during growth on LB agarose pads (LB = Luria Bertani). b, c) Super-resolution microscopy of *E. coli* (b) and *A. tumefaciens* (c) after short pulses with HADA. d) Super-resolution microscopy of *S. aureus* cells after a short pulse with HADA. Autofluorescence is shown in red. e) Triple labeling of *A. tumefaciens* with HADA (blue), EDA (clicked with red sulfo-Cy3-azide), and NADA (green). f) Triple labeling of *S. venezuelae* with NADA (green), TDL (red), and HADA (blue). Arrows in the triple-labeling panels indicate the sequence of labeling. White scale bars: 2 μm; red scale bars: 1 μm.

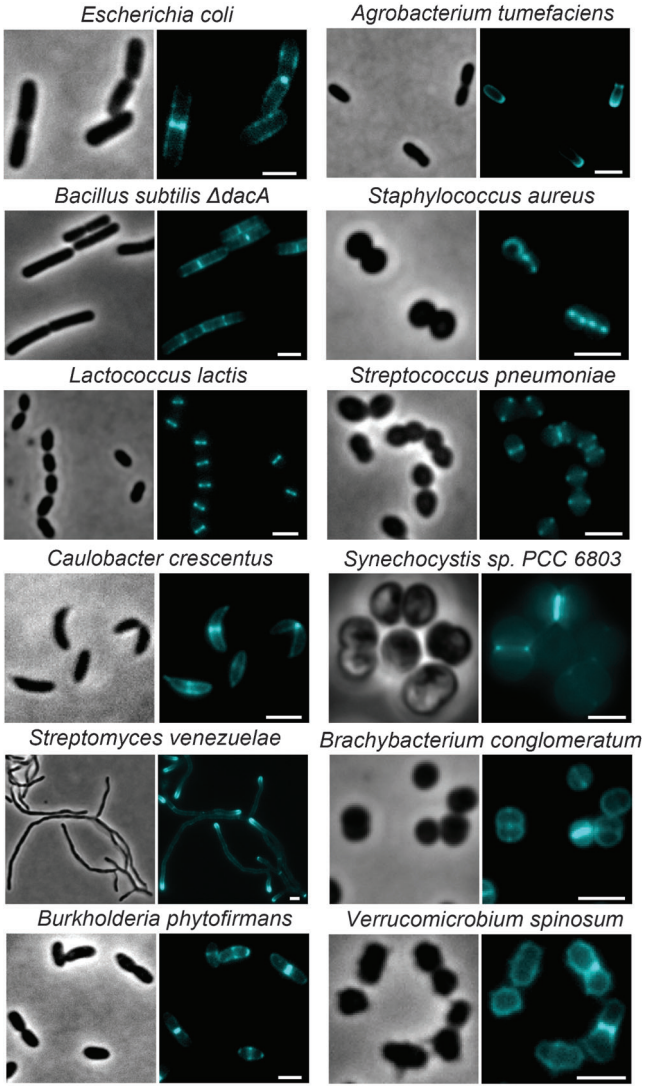

Figure 4. Short pulses of HADA label distinct modes of growth in diverse bacteria. Strains were labeled for ca. 2–8% of the doubling time: *E. coli* (30 s), *A. tumefaciens* (2 min), *B. subtilis ΔdacA* (30 s), *S. aureus* (2 min), *L. lactis* (2 min), *S. pneumoniae* (4 min), *C. crescentus* (5 min), *Synechocystis sp. PCC 6803* (1 h), *S. venezuelae* (2 min), *B. conglomeratum* (8 min), *B. phytofirmans* (20 min), *V. Spinosum* (10 min). Scale bars: 2 μm.

circumferential movement of the cell wall elongation machinery.[7] Short labeling times with *A. tumefaciens*, the growth of which occurs predominantly from a single pole and the site of cell division while the mother cell remains inert,[4] resulted in polar and septal labeling. Super-resolution fluorescence microscopy of labeled cells further enhanced the spatial resolution of the site of active PG synthesis (Figure 3c and Movie 4 in the Supporting Information).

PG labeling in three evolutionarily distant species suggested that FDAAs could specifically label the active site of PG synthesis across the entire bacterial domain. When species representing diverse phyla and modes of growth were briefly incubated with FDAAs, we observed strong labeling at the sites of cell division in actively dividing cells (Figure 4 and Figure S1b in the Supporting Information). This septal probe incorporation was the sole mode in *Synechocystis sp. PCC 6803*, *Lactococcus lactis*, and *Staphylococcus aureus* as previously described.[8] Super-resolution microscopy of *Staphylococcus aureus* further highlighted the different stages of these constricting septal rings (Figure 3d and Movie 5 in the Supporting Information). Labeling of *Streptococcus pneumoniae* occurred in single or split equatorial rings depending on the length of the cell, with peripheral labeling between the split rings as described.[8] Labeling of *Streptomyces venezuelae* was predominantly apical as reported,[9] with some weak labeling of vegetative septa and lateral walls, thus suggesting

a low but continuous lateral PG synthesis. In *Caulobacter crescentus*, labeling occurred at the sites of septal elongation, lateral elongation, and stalk synthesis, as reported elsewhere.[10]

Bacteria exhibit a myriad of growth patterns that provide selective advantages in the environment.[11] The strong correlation between FDAA labeling and previously inferred regions of new PG synthesis in diverse model species has a number of important implications. First, FDAA labeling marks the sites of active PG synthesis and therefore provides a long-sought broadly applicable tool to study the spatial dynamics of PG synthesis. Second, these results establish for the first time that the enzymes responsible for DAA incorporation in the PG are associated with active growth sites and that different areas on the surface of the sacculus are not equally accessible to these enzymes. Finally, FDAAs can be used to discover the growth modes of previously uncharacterized taxa. For example, our results show that *Burkholderia phytofirmans* exhibits polar and midcell PG synthesis, that *Brachybacterium conglomeratum* exhibits prominent peripheral PG synthesis in addition to seemingly alternating perpendicular division planes, and that *Verrucomicrobium spinosum* exhibits strong peripheral PG synthesis and asymmetric septal labeling (Figure 4).

The efficient label incorporation in all the bacteria studied thus far also suggests that FDAA incorporation, and therefore DAA incorporation, is common to the bacterial domain and FDAAs can thus be used to analyze natural bacterial populations, thereby providing a convenient and quick standard to measure bacterial activity and to probe the diversity of growth modes in complex microbiomes.[11] Indeed, labeling times with FDAAs as short as two hours revealed diverse modes of growth in saliva and freshwater samples in situ, but did not label dead cells as suggested by the strong correlation with live–dead staining (Figures S4b and S8 in the Supporting Information).

Encouraged by the efficiency of FDAAs, we sought to increase our toolkit for PG detection and modification using differently functionalized non-natural D-amino acids. By following a similar approach, we derivatized the brighter and more versatile core fluorophore, fluorescein (emission maximum ca. 515 nm, green), and its analogue, carboxytetramethylrhodamine (TAMRA, emission maximum ca. 565 nm, red),[12] with D-lysine to separate the bulky fluorophore from the DAA backbone, thereby generating FDAAs FDL and TDL (Scheme 1 and Figure S2a in the Supporting Information). Incubation of both *E. coli* and *B. subtilis* cells with FDL (536 Da) resulted in patterns similar to those with NADA, although labeling of *B. subtilis* was stronger than *E. coli*, presumably owing to reduced permeability of the *E. coli* outer membrane to molecules larger than approximately 500 Da[13] (Figure S9a–c in the Supporting Information). Indeed, the larger TDL (560 Da) did not label *E. coli* cells, but labeling of *B. subtilis* was prominent and gave patterns similar to other FDAAs (Figure S9a,b in the Supporting Information). To expand the toolkit further, we used "clickable" D-amino acids, namely ethynyl-D-alanine (EDA) or azido-D-alanine (ADA; Scheme 1), which can be specifically captured by using click chemistry by any molecule carrying the complementary functional group.[14] Similar to FDAAs, these bioorthogonal DAAs, but not the L-enantiomer control amino acid ELA, labeled both *E. coli* and *B. subtilis* cells when captured by commercially available azido/alkyne fluorophores (Figures S2c,d and S9d,e in the Supporting Information).

Furthermore, custom D-amino acids containing different colored fluorophores can be used sequentially to enable "virtual time-lapse microscopy." Since addition of each new probe indicates the location and extent of PG synthetic activity during the respective labeling periods, this approach provides a chronological account of shifts in PG synthesis of individual cells over time. This powerful method is exemplified here through click chemistry in gram-negative *A. tumefaciens* (Figure S1a in the Supporting Information and Figure 3e), or by the use of TDL in gram-positive *S. venezuelae* (Figure 3 f).

In contrast to the bacterial protein-making machinery's inherent bias against non-natural amino acids,[15] here we have shown that taxonomically diverse bacteria display a remarkable specific tolerance for incorporating D-amino acids with different sizes and functionalities into PG. By exploiting this tolerance we developed a rapid, nontoxic, and universal method for real-time tracking of PG at sites of active synthesis for the first time. Moreover, the combined utilization of two or more probes permits a temporal resolution that was never before achieved in cell wall growth studies. We expect that in combination with fluorescent fusion proteins, mutational analysis, and chemical perturbations, this methodology will allow a comprehensive analysis of the regulation and coordination of bacterial growth. Furthermore, the tolerance for DAAs with substantial sizes or with bioorthogonal handles will enable selective and specific modification of bacterial cell surfaces with various functionalities, thus paving the way for development of DAA-based bacteria-specific diagnostic or therapeutic probes. Finally, when cells labeled with FDAAs are hybridized with fluorescent in situ hybridization (FISH) probes, this approach will allow the culture-independent and concurrent measurement of growth (with FDAAs) and taxonomy (with FISH) and the response of bacteria to varying conditions in medical or environmental microbiomes.

Received: August 20, 2012
Published online: October 10, 2012

Keywords: bacteria · biosensors · D-amino acids · fluorescent probes · peptidoglycan

[1] A. Typas, M. Banzhaf, C. A. Gross, W. Vollmer, *Nat. Rev. Microbiol.* **2012**, *10*, 123 – 136.

[2] a) V. van Dam, N. Olrichs, E. Breukink, *ChemBioChem* **2009**, *10*, 617 – 624; b) R. A. Daniel, J. Errington, *Cell* **2003**, *113*, 767 – 776; c) K. Tiyanont, T. Doan, M. B. Lazarus, X. Fang, D. Z. Rudner, S. Walker, *Proc. Natl. Acad. Sci. USA* **2006**, *103*, 11033 – 11038; d) N. K. Olrichs, M. E. G. Aarsman, J. Verheul, C. J. Arnusch, N. I. Martin, M. Herve, W. Vollmer, B. de Kruijff, E. Breukink, T. den Blaauwen, *ChemBioChem* **2011**, *12*, 1124 – 1133; e) R. Sadamoto, K. Niikura, T. Ueda, K. Monde, N. Fukuhara, S.-I.

Nishimura, *J. Am. Chem. Soc.* **2004**, *126*, 3755 – 3761; f) M. A. de Pedro, J. C. Quintela, J. V. Höltje, H. Schwarz, *J. Bacteriol.* **1997**, *179*, 2823 – 2834.
[3] a) H. Lam, D.-C. Oh, F. Cava, C. N. Takacs, J. Clardy, M. A. de Pedro, M. K. Waldor, *Science* **2009**, *325*, 1552 – 1555; b) F. Cava, M. A. de Pedro, H. Lam, B. M. Davis, M. K. Waldor, *EMBO J.* **2011**, *30*, 3442 – 3453; c) T. J. Lupoli, H. Tsukamoto, E. H. Doud, T.-S. A. Wang, S. Walker, D. Kahne, *J. Am. Chem. Soc.* **2011**, *133*, 10748 – 10751.
[4] P. J. B. Brown, M. A. de Pedro, D. T. Kysela, C. Van der Henst, J. Kim, X. De Bolle, C. Fuqua, Y. V. Brun, *Proc. Natl. Acad. Sci. USA* **2012**, *109*, 1697 – 1701.
[5] H. L. Mobley, A. L. Koch, R. J. Doyle, U. N. Streips, *J. Bacteriol.* **1984**, *158*, 169 – 179.
[6] L. Furchtgott, N. S. Wingreen, K. C. Huang, *Mol. Microbiol.* **2011**, *81*, 340 – 353.
[7] a) J. Domínguez-Escobar, A. Chastanet, A. H. Crevenna, V. Fromion, R. Wedlich-Söldner, R. Carballido-López, *Science* **2011**, *333*, 225 – 228; b) E. C. Garner, R. Bernard, W. Q. Wang, X. W. Zhuang, D. Z. Rudner, T. Mitchison, *Science* **2011**, *333*, 222 – 225.
[8] a) R. Rippka, M. Herdman, *Ann. Inst. Pasteur/Microbiol.* **1985**, *136*, 33 – 39; b) A. Zapun, T. Vernet, M. G. Pinho, *FEMS Microbiol. Rev.* **2008**, *32*, 345 – 360.
[9] K. Flärdh, *Curr. Opin. Microbiol.* **2003**, *6*, 564 – 571.
[10] M. Aaron, G. Charbon, H. Lam, H. Schwarz, W. Vollmer, C. Jacobs-Wagner, *Mol. Microbiol.* **2007**, *64*, 938 – 952.
[11] K. D. Young, *Microbiol. Mol. Biol. Rev.* **2006**, *70*, 660 – 703.
[12] L. D. Lavis, R. T. Raines, *ACS Chem. Biol.* **2008**, *3*, 142 – 155.
[13] G. M. Decad, H. Nikaido, *J. Bacteriol.* **1976**, *128*, 325 – 336.
[14] J. A. Prescher, C. R. Bertozzi, *Nat. Chem. Biol.* **2005**, *1*, 13 – 21.
[15] a) H. Neumann, K. Wang, L. Davis, M. Garcia-Alai, J. W. Chin, *Nature* **2010**, *464*, 441 – 444; b) L. Wang, A. Brock, B. Herberich, P. G. Schultz, *Science* **2001**, *292*, 498 – 500.

